HUNGARIAN JOURNAL OF
INDUSTRY AND CHEMISTRY
Vol. 52(2) pp. 35–46 (2024)
hjic.mk.uni-pannon.hu
DOI: 10.33927/hjic-2024-17

COMPARISON OF THE WEAR AND FRICTION PROPERTIES OF TITANIUM NITRIDE-BASED COATINGS

OSAMAH IHSAN ALI[1,2], ISTVÁN GÁBOR GYURIKA[2], TAMÁS KORIM[1] AND MIKLÓS JAKAB[1*]

1 Department of Materials Engineering, Research Centre for Engineering Sciences, University of Pannonia, Egyetem u. 10, Veszprém, 8200, HUNGARY
2 Department of Mechanics, Research Centre for Engineering Sciences, University of Pannonia, Egyetem u. 10, Veszprém, 8200, HUNGARY

This paper describes the wear and friction behavior of titanium nitride (TiN)-based coatings produced via chemical vapor deposition (CVD) in detail. Coatings composed of TiN, titanium carbide (TiC) and aluminum oxide (Al_2O_3) layers were applied to a tungsten carbide-cobalt composite and steel substrates. The elemental and phase compositions of these coatings, manufactured with varying deposition parameters and layer thicknesses, were determined using scanning electron microscopy (SEM) and X-ray diffraction (XRD) analyses. The mechanical properties of the coatings were evaluated through Vickers microhardness testing, lubricant-free tribological model tests and scratch testing. For the linearly alternating tribological tests, a static counterpart made of yttria-stabilized zirconium oxide was utilized. The wear, friction and adhesive properties of the coatings were studied, revealing significant differences in tribological behavior based on their hardness, crystal structure and surface roughness. The tribological tests highlighted that coatings with sharp, spherical crystal structures on their surfaces exhibited the greatest resistance to abrasive and frictional stresses. The durability of the surface coatings was found to be primarily dependent on their adhesion and surface roughness.

Keywords: CVD, TiN, wear resistance, coating adhesion

1. Introduction

Surface treatments and coatings have become increasingly essential in addressing critical tribological challenges encountered in product design and when manufacturing machinery. Desired attributes include enhanced abrasion and wear resistance, favorable frictional behavior as well as reduced adhesion propensity coupled with substrate qualities such as toughness, machinability, cost-effectiveness and physical properties. However, the expanding array of commercially available treatments complicates the selection of optimal surface coatings. In order to effectively select them, comprehensive knowledge not only of the physical and mechanical properties as well as process characteristics of available coatings is required but also of their tribological performances under application-specific conditions [1]-[2].

Wear and friction behaviors are heavily influenced by the unique tribological system of each application, incorporating factors such as loading conditions, velocity, relative surface movements, lubrication, temperature and the atmosphere. While the specifics vary, laboratory tribological tests conducted under controlled conditions offer valuable insights into anticipated real-world performance. Nonetheless, discrepancies in experimental procedures and conditions from published data hinder a reliable comparison of the tribological behaviors of coatings [3]-[5].

To address this challenge, a series of unlubricated-sliding pin-on-disk tests were conducted at a constant sliding speed as well as loading and atmospheric conditions. The primary aim was to collect data facilitating the selection of surface coatings for unlubricated sliding bearing-surface applications. Coatings produced via physical vapor deposition (PVD), chemical vapor deposition (CVD) and plasma spray (PS) techniques were tested individually and in combination with each other as well as with an uncoated hardened steel tool to examine the impact of the coating on the wear of the steel [6].

In the realm of metal forming, cutting tools composed of cemented carbide (tungsten carbide (WC) with Co binder phase) have long been favored. However, concerns over the toxicity of cobalt have prompted the search for alternative materials in the binder phase like Fe and Ni. Meanwhile, escalating demands for quality and productivity underscore the imperative for high-performance tools [3],[7].

To augment the wear resistance of cutting tools, hard protective coatings, typically applied via CVD or

Received: 6 June 2024; Revised: 20 June 2024;
Accepted: 20 June 2024
*Correspondence: jakab.miklos@mk.uni-pannon.hu

PVD, are employed. CVD-coated WC-Co cutting tools often feature a multilayer system comprised of titanium nitride - titanium carbonitride - aluminum oxide (TiN-TiCN-Al_2O_3) with titanium nitride (TiN) serving as the innermost layer [8]. However, changes in the WC-Co binder phase necessitate an investigation into the interactions between the gas phase and the new binder to maintain coating-substrate performance. CVD of TiN onto various potential binder phases such as Ni and stainless steel has been studied, revealing variations in growth rate, texture and coating morphology. The adhesion of TiN coatings may also be affected by diffusion of the binder-phase material into the coating. Studies have shown that substrates containing Co exhibit superior tool-coating adhesion compared to Fe and Ni-based substrates. While porous coatings typically exhibit inferior mechanical properties unsuitable for metal cutting applications, the growth of CVD of TiN on Ni surfaces has demonstrated porous characteristics, potentially due to the interaction between $TiCl_4$ and Ni forming Ni chlorides in the gas phase. Understanding such interface chemistry during CVD of TiN can help suppress the formation of intermetallic phases, thereby enhancing mechanical properties conducive to cutting tool applications [9].

Titanium nitride (TiN) coatings are commonly applied to cemented tungsten carbide cutting tools using a hot-wall CVD reactor, employing mixtures of $TiCl_4$, N_2, H_2 and Ar. The deposition reaction yields solid TiN and gaseous HCl, thermodynamically favored above approximately 750 °C at atmospheric pressure. While $TiCl_4$ and N_2 provide coating components, H_2 facilitates the reduction of $TICl_4$ while Ar enhances gas mixing and serves as a carrier gas to achieve reasonable deposition rates. Although the process typically operates at atmospheric pressure, low-pressure CVD of TiN has been demonstrated. The gases, introduced at room temperature, are rapidly heated within the reactor which is maintained at 900-1200 °C. Deposition rates of 0.03-0.20 µm min^{-1} are achieved under these conditions [10].

The CVD process, conducted at temperatures ranging from 950 to 1050 °C, known as high-temperature CVD (HT-CVD), synthesizes TiCN coatings with small equiaxed crystals. The composition of Ti(Cx,Ny) grains can be adjusted to achieve various C/N ratios, crucial for optimizing coating properties while increasing cutting speeds. The morphology, orientation and size of grains as well as the presence of defects significantly influence coating properties. Controlling crystallite size and morphology is achievable by adjusting CVD parameters and doping with species like H_2S, CO, CO_2 or $ZrCl_4$ [11]-[12].

Zheng et al. [13] demonstrated control over the grain morphology and hardness of TiN wear-resistant coating layers by manipulating the $(H_2+N_2)/TiCl_4$ ratio at a specified CVD temperature. Fieandt et al. [14] proposed improving the chipping resistance of coatings by precisely controlling the distribution of C and N atoms in the crystal lattice of TiCN coatings. Reducing grain size is desirable as nanocrystalline coatings exhibit superior wear resistance attributed not only to the Hall-Petch relationship but also to grain boundary effects like dislocation and strain hardening.

A vacuum-tight chamber heated by resistance or radiation from high-temperature materials like graphite or Kanthal Super® is typically used. Cutting tools are densely packed onto trays and stacked to form a load that nearly fills the chamber. The temperature is precisely controlled using a multizone heater, facilitating temperature ramping in the direction of the gas flow to achieve faster reaction rates. Commercial CVD reactors for coating cutting tools incorporate subsystems to facilitate a vacuum, gas handling and scrubbing as well as process control, often operated by software, which minimizes the need for human intervention [15]. Various modifications to the process have been introduced, e.g. interrupting film deposition to promote the nucleation of finer-grained layers in addition to using dopants like $AlCl_3$ to reduce grain size as well as enhance the strength and lifespan of the coating [16]. Plasma-enhanced CVD processes have also been explored, depositing coatings at lower temperatures and consuming less gas, in spite of complexities. Additionally, low-temperature CVD of TiN has been demonstrated, yielding coatings at temperatures as low as 40 °C, albeit with low densities and high impurity content, hindering adhesion and performance. Studies on the kinetics of CVD of TiN have identified temperature-dependent rate-controlling steps, typically assumed by modeling due to difficulties in making direct measurements. These studies have provided insights into the influence of precursor concentrations and reaction mechanisms on deposition rates, aiding the optimization of process parameters for specific reactor configurations. However, the transferability of findings between reactors remains a challenge due to reactor-specific conditions [17]-[18].

Nevertheless, research continues to refine CVD processes to enhance the properties and performance of TiN coatings. Investigating these coatings in terms of mechanical properties, chemical composition and structure helps to select optimal coatings for specific industrial applications. Tribological tests are crucial to evaluate changes in the coefficient of friction, the adhesion of coatings to substrates and abrasion resistance. Understanding the wear process by carrying out detailed investigations of worn surfaces is vital to enhance the wear resistance of machine elements and tools. The "pin-on-disk" test is a commonly used method to assess tribological properties, simulating wear through contact and relative rotation. This study aimed to analyze the tribological properties of hard, wear-resistant coatings produced by CVD on tungsten carbide and steel substrates.

2. Materials testing methods

A morphological analysis was performed utilizing an Apreo S by ThermoFisher Scientific (formerly FEI) scanning electron microscope (SEM) in a high vacuum, employing an accelerating voltage of 20.0 kV. Prior to observations, the samples were cleaned in an ultrasonic

Table 1: Abbreviations and the type of CVD coatings investigated

Sample	Layer type	Substrate	Thickness (μm)		
			Layer 1	Layer 2	Layer 3
TiN1	single layer	WC	0.3-0.6		
TiN2	single layer	WC	0.7-0.9		
TiN3	single layer	WC	1.8-2.8		
TiN4	single layer	WC	2.9-3.8		
TiN5	single layer	WC	5.8-7.2		
TiN6	single layer	WC	6.3-7.8		
TiC/TiN	two-layer	WC	1.2-1.4	1.5-3.1	
TiCN/Al/TiN	multi-layer	WC	8.1-8.6	2.2-3.1	0.9-1.1
TiCN	single layer	ST	0.5-0.7		

bath containing ethanol and acetone to optimize resolution for back-scattered electron imaging. The images were taken by a Keyence VHX-2000 digital light microscope. Cross-sections were prepared by embedding samples in epoxy resin (NX MET XF40) before being polished. The elemental compositions were determined using an EDAX AMETEK Octane Elect Plus energy dispersive X-ray analyzer with an accelerating voltage of 20 kV and a data collection time of 180 s.

A microhardness assessment was conducted on both the coated and uncoated (reference) samples using the Vickers microhardness method (4.903 N, Wolpert 402 MVD) with a loading force of 0.05 kgf. The hardness values were determined as the average of five readings per specimen. The indentation diameter measured during hardness testing can be used to calculate the penetration depth of the diamond pyramid. The geometry of the diamond pyramid is known based on the manufacturer's datasheet. By determining the penetration depth, it is clear whether the measured hardness pertains solely to the coating and if the hardness of the substrate also influences it.

The X-ray diffraction (XRD) analyses were conducted using a Philips PW 3710 diffractometer with Cu-K α radiation (50 kV, 40 mA), employing a scan rate of 0.02 2θ/s over a range of 10 to 70 degrees 2θ and incorporating a curved graphite monochromator. XRD pattern data were collected using X'Pert Data Collector software, while phase identification and quantitative phase analysis were performed utilizing HighScore Plus 5.0 software using the Rietveld method. The crystalline phases were identified by comparing XRD patterns with the 2021 Powder Diffraction Files (PDF-2 2021) from the International Centre for Diffraction Data (ICDD).

The tribological performance was evaluated through dry-sliding experiments utilizing an Anton Paar TRB3 tribometer in a ball-on-disc configuration, following standards ASTM G99-05 [19] and ASTM G133-05 [20]. Coatings were subjected to tests against steel balls 6 mm in diameter (Anton Paar, 100Cr6 steel ball) and zirconia balls 5 mm in diameter (Max Fritsch, zirconium oxide grinding ball) at 25 °C in ambient air with a relative humidity of 46±3%. The maximum sliding speed and normal load were maintained at 15.71 cm/s and 20 N, respectively. The coefficient of friction (μ) was continuously monitored in relation to the sliding distance. Following tests, the wear track was cleaned with alcohol to remove loose wear debris and subsequently measured using a profilometer. The wear volume (Vp, mm^3) values were then calculated in accordance with the aforementioned standards to compare the wear resistance of the coatings.

$$Vp = (\pi h/6)[3D^2/4 + h^2] \quad (1),$$

where h denotes the height of the removed material from the ball (mm) and D represents the diameter of the wear scar on the ball. The height of the material removed can be calculated as follows:

$$h = R - [R^2 - (D^2/4)]^{1/2} \quad (2),$$

where R denotes the original radius of the ball (mm).

A customized scratch test methodology was employed to assess the adhesion of the coating. The examination utilized an Anton Paar TRB3 tribometer with a fixed total stroke length of 10 mm and a consistent normal force of 5 N. Diamond indentation marks left on the surface were scrutinized via SEM. Furthermore, the surface roughness was analyzed using a Taylor Hobson/AMETEK Surtronic S-128 surface roughness tester.

A C-Therm TCi™ thermal conductivity analyzer was used to determine the thermal conductivity of the test samples. The heating element was heated to 150 °C, the heat pulse lasted for 3 seconds and the total measurement time was 7 seconds. Five parallel measurements were conducted. In each case, distilled water was used as a contact agent.

3. Results and discussion

The samples examined during the experimental work and their abbreviations are summarized in *Table 1*. The titanium nitride-based coatings were produced with varying manufacturing parameters, including the volumetric flow rate of precursors, temperature and

Table 2: The atomic percentage composition of substrates and the different types of coatings

	WC	ST	TiN1	TiN2	TiN3	TiN4	TiN5	TiN6	TiC/TiN	TiCN/Al/TiN	TiCN
W	30.5±1.1		0.2±0.1	0.5±0.1	3.7±0.2	0.8±0.2			0.8±0.2		
Co	8.6±0.5		0.3±0.1		10.4±0.3	1.9±0.1			0.7±0.2		
C	55.6±5.9	0.8±0.2							33.1±1.2		21.6±2.1
O	4.7±0.7		2.1±0.2	0.8±0.1		1.2±0.1				6.3±0.6	
Ti			62.1±0.7	50.6±0.7	31.6±0.6	53.7±0.2	59.1±0.8	54.5±0.8	30.9±0.4	34.8±0.6	8.9±0.2
N			33.5±2.1	48.1±3.7	54.3±4.1	42.5±0.8	40.9±2.5	45.5±2.6	36.4±1.3	49.8±3.5	24.1±2.2
Fe		98.6±1.9									45.1±0.9
Mn		0.3±0.1									0.2±0.1
Cr	0.6±0.2	0.3±0.2							0.9±0.2		0.2±0.1
Al										9.2±0.6	

pressure. The test specimens presented in the study were produced by Büttner Kft. (Nagyatád, Hungary) in a newly developed reactor located at their site. Tungsten carbide-cobalt cermet and steel were used as substrates for the coatings. One of the most important parameters in this experiment is the thickness of the deposited layers. To determine the layered structure, the samples were embedded in epoxy resin and polished with various grades of abrasive papers. The final polishing step was performed with a suspension containing diamond particles 3 µm in diameter. After polishing, the layer thicknesses were measured using SEM.

Six different samples of titanium nitride-based coatings were examined during the work with thicknesses ranging from 0.3 to 7.8 µm. For the WC-Co substrate coated with layers of titanium carbide and titanium nitride, the main goal was to study the effect of the titanium carbide layer on the tool life in a similar manner to the sample containing the layer of aluminum oxide support. The purpose of examining the steel sample was to study the tribological properties of the coating less than 1 micrometer thick.

3.1. Microstructure and composition

The atomic percentage composition of the surfaces is summarized in *Table 2*. Before being examined by energy-dispersive X-ray analysis, the samples were cleaned in an ultrasonic bath with acetone for 5 minutes and then wiped with a lint free cloth. The elemental composition on the surfaces of the samples was determined over areas of approximately 1 mm^2. For each specimen, three parallel measurements were taken.

The elemental composition of the WC-labeled substrate shows that, in addition to the WC-based crystalline phases, it contains chromium and cobalt binders. The steel-based substrate (ST) primarily consists of iron with small amounts of alloying elements such as carbon, manganese and chromium, indicating that the substrate is a wear-resistant steel alloy.

The elemental composition of the titanium nitride-based coatings reveals that they mainly contain titanium and nitrogen with varying atomic percentage ratios depending on the manufacturing parameters. However, for samples TiN1-TiN4, characteristic X-ray peaks indicative of the substrate were also observed in the energy-dispersive spectra, suggesting that the excitation (information) volume depth caused by the electron beam is greater than the thickness of the coating. Samples TiN1 and TiN3 contain relatively high cobalt concentrations, implying that cobalt diffused to the surface due to the high temperatures used during coating deposition [21], potentially affecting the structure of the coating as well as its wear and friction properties. When the coating thickness exceeded 5 µm, elements indicative of the substrate were no longer detectable in the composition.

The results from the X-ray diffraction analysis of the coatings are summarized in *Table 3*. Similar to the findings from the elemental composition analysis, reflections characteristic of the different types of substrate were observed alongside the reflections from the crystalline phases of the coating. For the titanium nitride-based coatings, the primary crystalline phase is TiN in all cases. However, depending on the manufacturing parameters, samples TiN1, TiN2 and TiN4 also exhibit reflections characteristic of the TiO crystalline phase. This indicates that the vacuum or the flow rate of the precursors during production was not perfect, causing partial oxidation of the coating at high temperatures, thereby adversely affecting the desired coating quality. For the two-layer coating, it is evident that one of the main components of one layer is the TiN crystalline phase, while the other layer is comprised of a TiCN crystalline phase. In the case of the coating reinforced with an aluminum oxide phase, reflections characteristic of Al_2O_3 are present. For the steel-based sample, reflections corresponding to the crystalline phases typical of steel are observed.

The microstructure of various types of coatings is illustrated in *Figure 1*. It is evident that the TiN crystalline phases in samples TiN1 (*Figure 1a*), TiN2 (*Figure 1b*), TiN3 (*Figure 1c*) and TiN4 exhibit a

Table 3: The phase composition of the substrates and coatings

JCPDS card number	Phase	WC	ST	TiN1	TiN2	TiN3	TiN4	TiN5	TiN6	TiC/ TiN	TiCN/ Al/TiN	TiCN
01-085-4359	WC	x		x	x	x	x	x	x	x	x	
01-089-7373	Co	x		x		x	x	x	x	x	x	
01-089-2005	Fe_3C		x									x
00-006-0696	Fe		x									x
00-051-0997	Fe_5C_2		x									x
01-074-8388	TiN			x	x	x	x	x	x	x	x	
03-065-9875	$TiC_{0.496}N_{0.502}$									x		x
00-008-0117	TiO			x	x		x				x	
00-023-1455	Ti_2N				x							
03-065-4761	W_5N4			x						x		
00-026-0031	Al_2O_3										x	

Table 4: Vickers-hardness (in HV) of the samples

	WC	ST	TiN1	TiN2	TiN3	TiN4	TiN5	TiN6	TiC/ TiN	TiCN/Al/ TiN	TiCN
Value 1 (HV)	1801	226	2027	1850	2119	2250	1709	1810	1875	3093	238
Value 2 (HV)	1900	238	2246	2189	2181	2119	1668	1790	1983	3203	162
Value 3 (HV)	2122	130	1874	1983	1889	2092	1862	1785	2249	2889	170
Av. (HV)	1941.1	198.0	2049.0	2007.3	2063.0	2153.7	1746.3	1795.0	2035.7	3061.7	190.0
Sd. (HV)	164.4	59.2	187.0	170.8	153.8	84.5	102.2	13.2	192.5	159.3	41.8
Hardness (GPa)	19.0	1.9	20.1	19.7	20.2	21.1	17.1	17.6	20.0	30.0	1.9
Pd (µm)			2.1	2.4	2.7	5.1	2.9	4.0	2.4	2.0	10.4

Av.: average of the Vickers-hardness values 1-3, *Sd.*: standard deviation of Vickers-hardness values 1-3, *Pd*: penetration depth

predominantly spherical morphology. In these cases, the layer thickness is less than 4 µm. Although samples TiN1, TiN3 and TiN4 are composed of spherical crystals of similar size, these crystals are much more densely packed on the surface of sample TiN4. The crystals in sample TiN2 are smaller compared to the others. Previous studies indicate that these spherical crystals form when the coating temperature is below 990 °C. In sample TiN3, the spherical crystals appear slightly elongated, likely due to cobalt diffusion. Samples TiN5 and TiN6 display star-shaped and lenticular-like crystals, which form at reaction temperatures above 1050 °C. The TiN/TiC sample exhibits star-shaped and rounded particles on its surface, which typically form around 990 °C [4],[12]. The multi-layered sample also exhibits spherical and lenticular-like crystals, whereas the coating on the steel substrate does not show distinctive crystal shapes, only a few spherical crystals on the surface.

The hardness of the coatings (*Values 1, 2 and 3*) and the penetration depth (*Pd*) of the diamond pyramid are summarized in *Table 4*. The results show that the coatings on the WC substrate generally increased the hardness of the test specimens. However, a decrease in hardness is observed in samples TiN5 and TiN6. As seen in the SEM images (*Figure 1*), these coatings consist of plate-like crystals that fill the available area less effectively, resulting in higher porosity and lower hardness values.

For samples TiN1-TiN4 and TiCN, since the penetration depth exceeds the coating thickness, this phenomenon must be considered when interpreting the data. Nonetheless, the SEM images clearly show that the spherical and star-shaped crystals cover the surface more uniformly compared to the lenticular-like ones. The effect of the CVD coating on the hardness of the steel substrate could not be measured as the coating thickness is less than 1 µm and the penetration depth on the relatively soft steel greater than 10 µm. Consequently, the measured hardness essentially reflects the hardness of the steel itself.

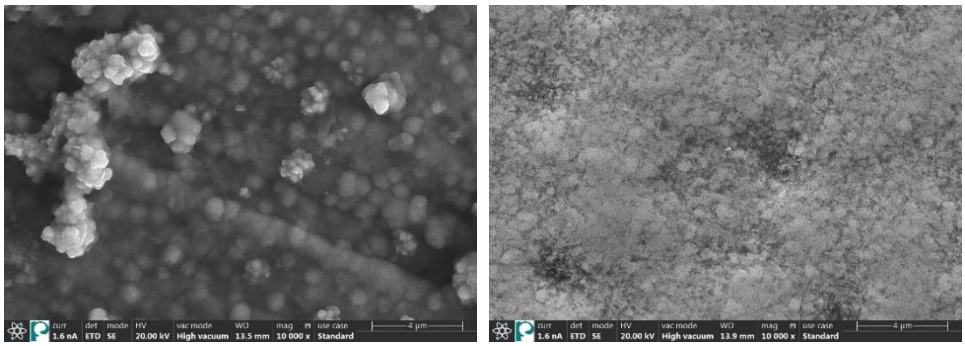

a) TiN1 b) TiN2

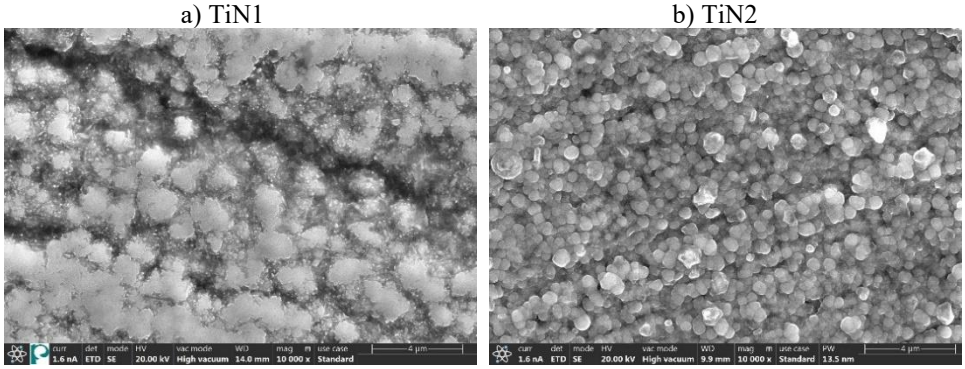

c) TiN3 d) TiN4

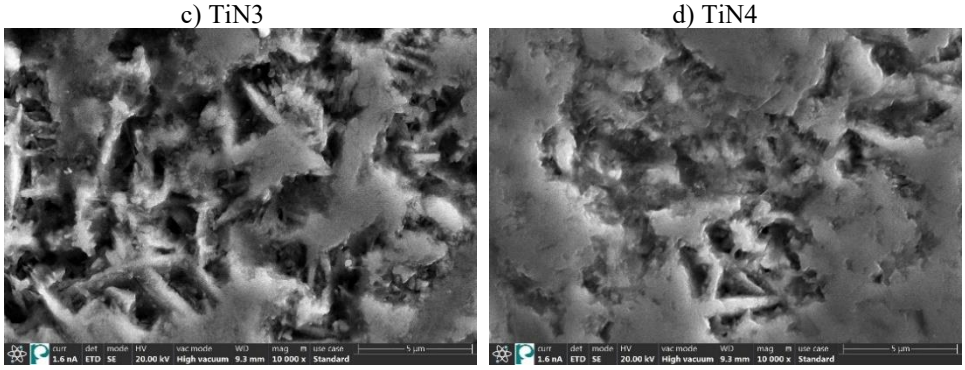

e) TiN5 f) TiN6

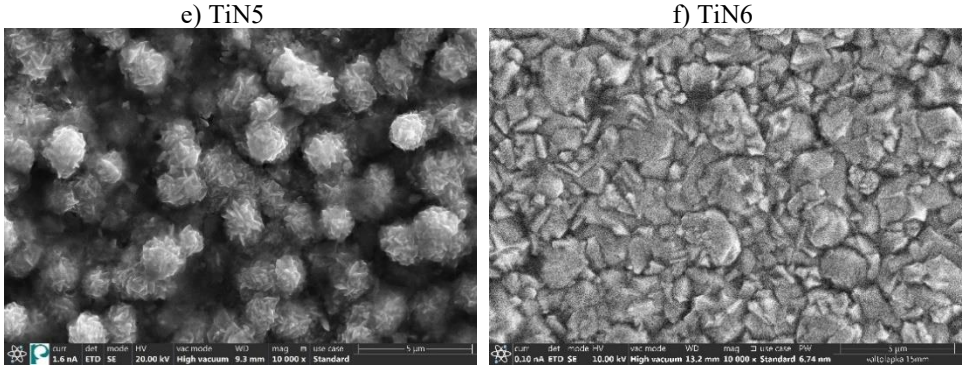

g) TiN/TiC h) TiCN/Al/TiN

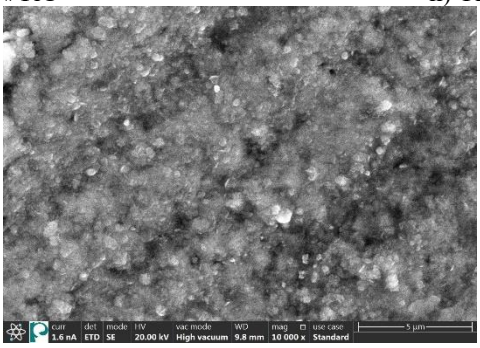

i) TiCN

Figure 1: Microstructure of the coatings

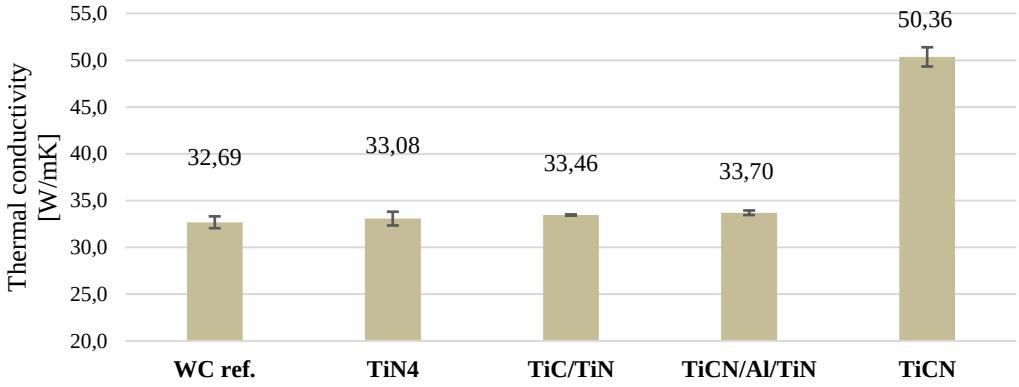

Figure 2: Thermal conductivity of the samples

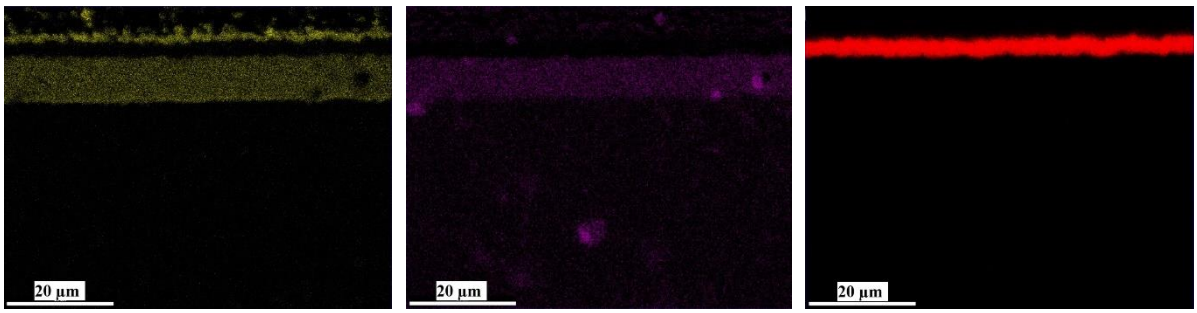

Figure 3: Elemental map of the cross-section of the TiCN/Al/TiN sample where yellow indicates nitrogen (a), purple indicates carbon (b) and red indicates aluminum (c)

The thermal conductivity of various types of coatings is summarized in *Figure 2*. The WC-Co samples exhibit fundamentally lower thermal conductivities compared to those measured for steel. For the test specimens coated with TiN and TiC/TiN, the coating thickness was nearly identical, but a slight increase in thermal conductivity was observed compared to the reference values. The coating that included a corundum layer exhibited the highest thermal conductivity among the WC-Co samples. For the steel-based test specimen, the highest measured value was 51.2 W/mK. When interpreting the results, the measurement error due to irregularities in the surface of the test specimens must be considered. As observed in the SEM images, air gaps between the spherical surface particles can affect the measured thermal conductivity of the coated products. Based on the thermal conductivity values, it can be concluded that using WC-Co composites as machining tools is advisable as these typically have lower thermal conductivities, thereby heating up less during machining.

3.2. Tribological behavior

To determine the experimental parameters for the tribological model tests, a test specimen with a TiCN/Al/TiN composite coating was used. The layer structure is illustrated in the elemental map in *Figure 3*, which clearly shows that the layer closest to the substrate contains both nitrogen and carbon, indicative of the TiCN layer. This is followed by an aluminum-containing support layer and then an upper titanium nitride layer. According to the results presented in *Table 1*, the thickness of the upper titanium nitride layer is approximately 1 µm.

In the first step of the tribological investigations, a steel ball 6mm in diameter was used as the static counterpart. During the measurements, the degree of displacement was 10 mm, the maximum speed of the coated sample 15.71 cm/s and the total distance covered 500 m. Throughout the experimental series, the normal compressive forces applied were 10, 20 and 60 N. In the measurement conducted with a loading force of 10 N, it was observed that the steel used as the static counterpart smeared onto the surface and, after a certain time, the wear and friction mechanism became uninterpretable. This phenomenon indicates that over time, wear surfaces of steel-on-steel were formed rather than measuring the wear of the coating. Even though the experiment was repeated with higher normal compressive forces (20 and 60 N), similarly to the previous attempts, the wear surface was not evaluable (*Figure 4a*). Subsequently, the surface was washed with an 18 vol.% hydrochloric acid solution to remove the smeared steel layer as shown in *Figure 4b* from which it is evident that the wear surfaces are virtually identical. Furthermore, despite increasing the normal compressive force, the approximately 1 µm-thick TiN coating was not removed, even after the 500 m long test.

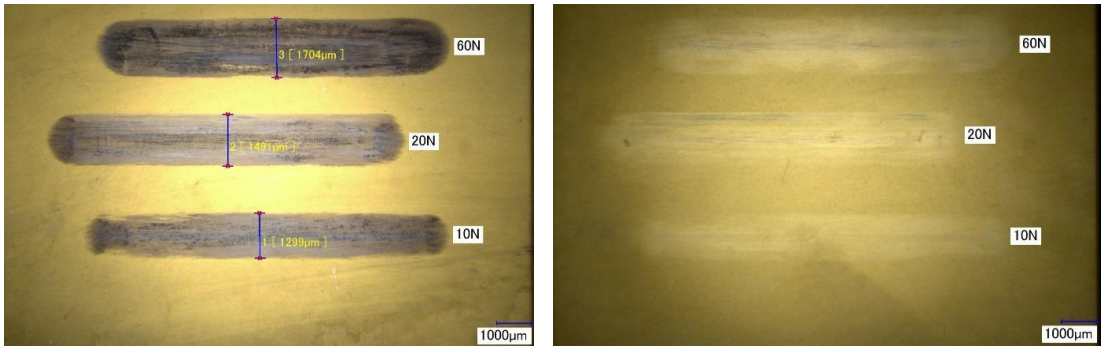

a) b)

Figure 4: LM images after the experiments conducted with the steel test specimen where (a) denotes the smeared steel and (b) denotes the surface of the sample after hydrochloric acid cleaning

The experiments conducted with the steel static counterpart confirmed that using a material system with a hardness comparable to that of the coating under investigation is advantageous regarding the tribological analysis of titanium nitride and titanium carbide-based coatings [22]-[24]. In this regard, yttrium-stabilized zirconium dioxide balls were subsequently employed with a hardness of 13-14 GPa [25]. In this case, the hardness of the static counterpart is slightly lower than that of the coatings. However, this setup allows for the examination of the wear track formed due to wear and friction effects as well as of the volume removed from the contact surface of the ball. Accordingly, further investigations were conducted with ZrO_2-based static counterparts using the previously described measurement parameters. The normal compressive force applied in each case was 20 N.

To interpret the wear and friction conditions, the diameter of the circular wear track formed on the bottom of the contact surface of the ZrO_2 ball due to wear (D) was measured using a light microscope. With D and the radius of the ball (R=2.5 mm) known, the wear height of the static counterpart (h) could be calculated using *Equation 2* before calculating the wear volume (Vp) using *Equation 1*.

The results obtained are summarized in *Table 5* in which the last column shows the average surface roughness (Ra) specific to each sample. The surface roughness and crystalline structure formed on the surface also have a significant impact on tribological properties. The coefficient of friction was periodically recorded using Anton Paar TRB3 Version 9.0.16. software. Should this coefficient increase, it can be inferred that abrasive particles have moved between the contact surfaces, causing abrasion to both the zirconium oxide ball used and the sample surface. First signs of the abrasive wear effect were noticed when the coefficient of friction reached 0.5. From the known measurement time and speed, the distance traveled could be calculated, after which it was presumed that the coating probably had detached from the sample surface.

To confirm the detachment of the surface layer from the wear track, energy-dispersive X-ray analysis was performed. According to the results, sample TiN2 exhibited the smallest surface roughness and wear volume with a layer thickness of 0.7-0.9 µm.

Table 5: Reduction in wear volume and average surface roughness

Sample	D (mm)	h (mm)	Vp (mm^3)	Vp (μm^3)	Ra (µm)
TiN1	0.440	4.84E-03	3.68E-04	3.68E+05	0.61
TiN2	0.268	1.80E-03	5.07E-05	5.07E+04	0.16
TiN3	0.567	8.04E-03	1.02E-03	1.02E+06	0.25
TiN4	0.470	5.53E-03	4.79E-04	4.79E+05	0.56
TiN5	0.505	6.38E-03	6.39E-04	6.39E+05	0.36
TiN6	0.498	6.20E-03	6.04E-04	6.04E+05	0.34
TiC/TiN	0.389	3.78E-03	2.25E-04	2.25E+05	0.39
TiCN/Al/TiN	0.609	9.28E-03	1.35E-03	1.35E+06	0.33
TiCN	0.541	7.32E-03	8.42E-04	8.42E+05	0.74

D: diameter of the wear scar on the ball, h: height of the removed material from the ball, Vp: wear volume, Ra: average surface roughness

In this case, based on the energy-dispersive X-ray spectroscopy (EDS) results, the coating did not wear off during the test. Although the coefficient of friction exceeded μ=0.5 after 30 m, the abrasive particles did not abrade the surface. Similar results were observed for the TiC/TiN, two-layered sample as well. The average surface roughness in this case was more than double that measured for sample TiN2 and the wear volume nearly an order of magnitude higher. As seen in *Figure 1*, the surface of this sample consists of sharp crystals in the TiN layer, which have a particularly good abrasive effect. However, while measuring the elemental composition, it was observed that the coating did not detach from the surface. In this case, signs of abrasion appeared on the time-coefficient of friction diagram after 4.7 m. Although the coefficient of friction continued to increase steadily throughout the remaining measurement time, no further layer detachment was observed. For sample TiN4, the coefficient of friction exceeded 0.5 after 204.9 m. Based on the EDS results, in this case, the 2.9-3.8 µm-thick coating did not wear off during the tests. Samples TiN5 and TiN6 behaved similarly during the tribological tests. Detachment of abrasive particles was first noticed after traveling 7.2 and 7.8 m, respectively. The coefficient of friction remained constant throughout the experiment (μ_{max}=0.95). For the TiCN/Al/TiN sample, signs of detachment of the top layer were visible after 7.1 m. Based on the EDS results, only the upper ~1 µm-thick TiN layer partially detached, while the underlying aluminum oxide layer remained intact. However, the wear volume was the highest in this case, indicating that although the TiN layer partially wore off the surface, the abrasive effect of the coating continued during the test. In the case of samples TiN1 and TiN3, the coating completely wore off. For sample TiN1, with a coating thickness below 1 µm, it fully detached from the surface after 1.3 m. For sample TiN3, the coating likely detached after 150 m according to the tribological test.

The steel substrate coated with a TiCN layer exhibited the highest surface roughness but the coating wore off the surface after 15.4 m. Subsequently, the coefficient of friction remained constant throughout the test, indicating that the zirconium oxide ball only abraded the steel substrate.

The effect of surface roughness and microhardness on wear volume is illustrated in *Figures 5* and *6* from which it is evident that in the case of stable coatings, that is, those that did not wear off, the coefficient of friction

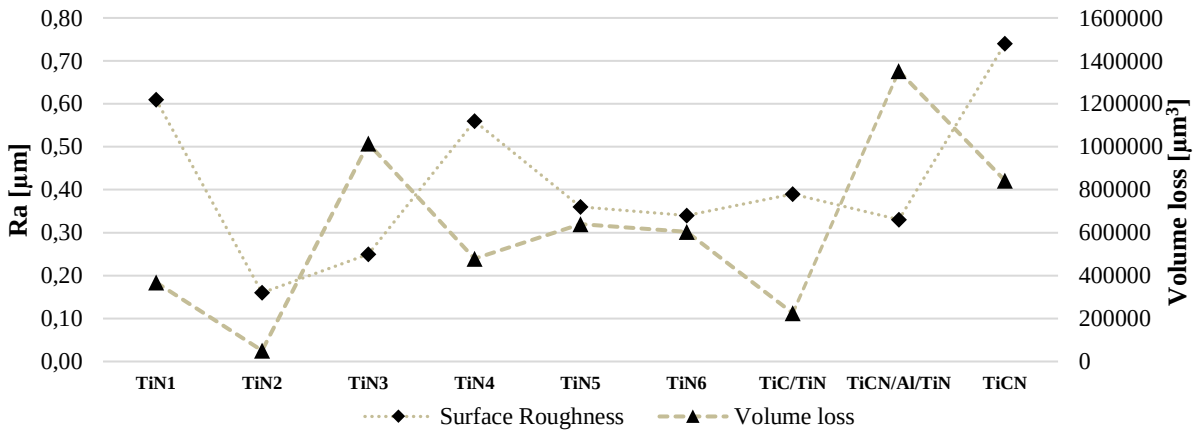

Figure 5: The effect of average surface roughness on wear volume

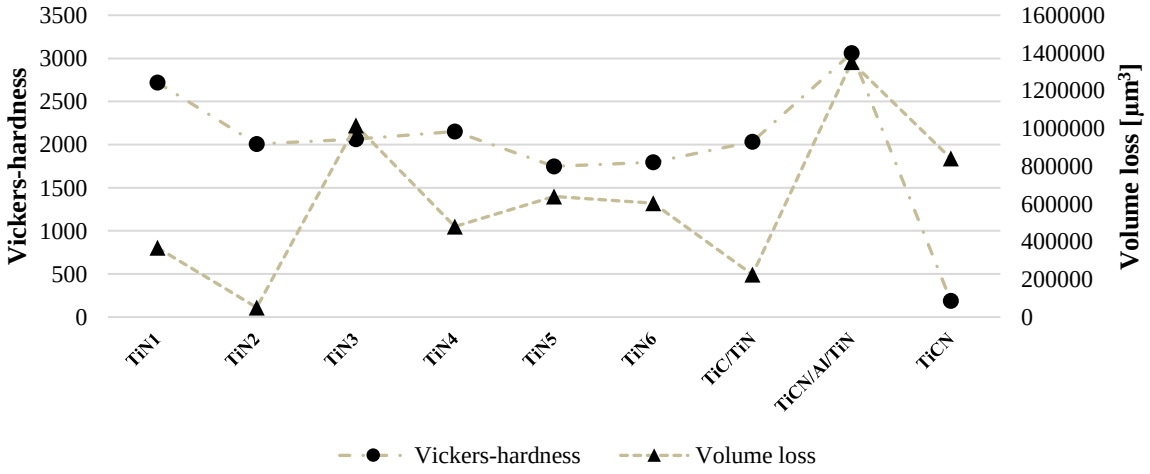

Figure 6: The effect of microhardness on wear volume

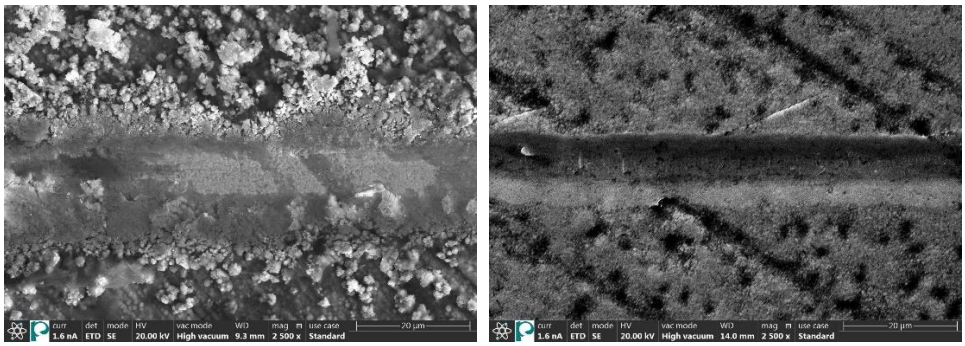

a) TiN1 b) TiN2

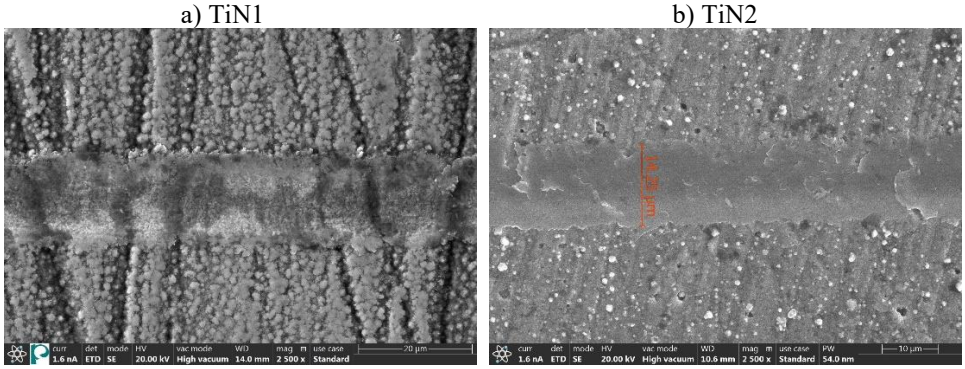

c) TiN3 d) TiN4

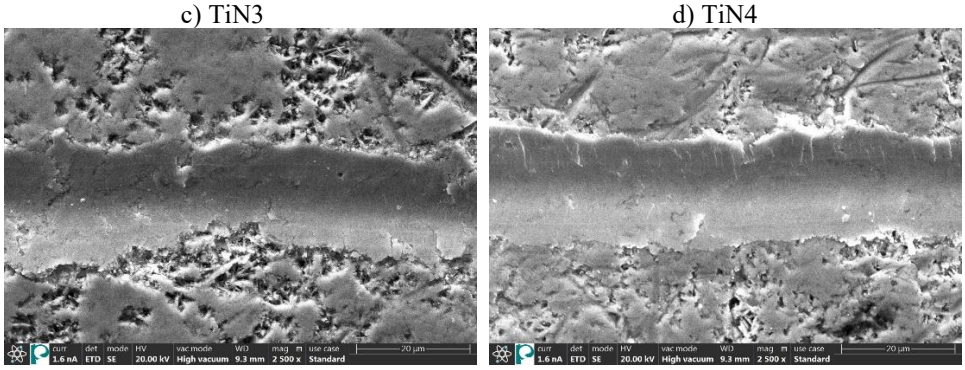

e) TiN5 f) TiN6

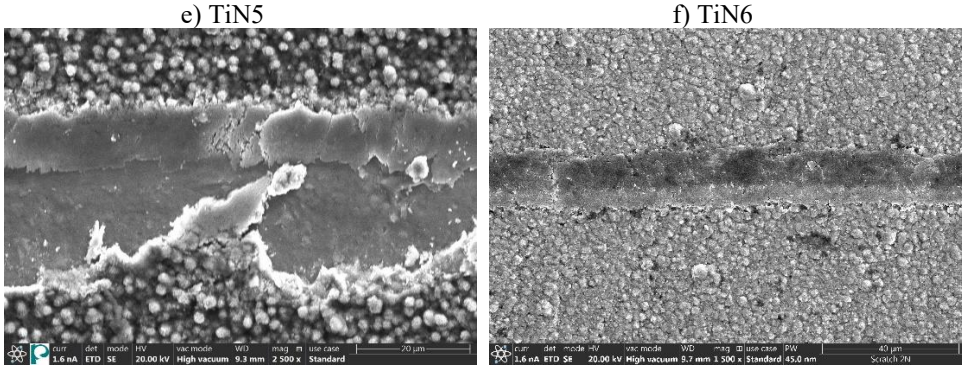

g) TiN/TiC h) TiCN/Al/TiN

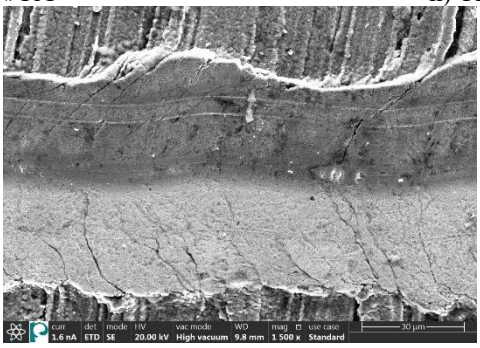

i) TiCN

Figure 7: Scratch test-induced scratch tracks on the surfaces of the test samples

and wear volume changed analogously. However, no similar observation was made regarding hardness. A good example of this is seen in the TiN2 and TiCN/Al/TiN samples, where the surface roughness is the lowest among the samples examined, however, their wear volume differs significantly. Therefore, from a tribological perspective, in TiN-based systems, it is advantageous for the coating to be fairly dense, exhibit a low degree of porosity as well as have surface roughness and hardness values significantly greater than those of the applied counterpart or the tools in the case of the test specimen being machined. In terms of tribology, apart from the wear and friction conditions, adhesion of the coating to the surface is crucial. For this purpose, a custom-developed scratch test was employed during which a diamond stylus with a geometry similar to that used for Vickers hardness testing was drawn along the surface of the test samples over a length of 10 mm while applying a normal load of 2 N.

As depicted in *Figure 7*, the coating flaked off along the scratch line of the TiN1 and TiC/TiN samples, indicating poor adhesion of the coating to the surface, which is significant in the case of the bilayer coating that exhibited favorable properties during tribological tests, however, adhesion of the layer is weak. The least amount of deformation was observed in the TiN2 and TiCN/Al/TiN coatings. In these cases, as evident from the diameter of the scratch, the stylus did not penetrate deeply into the surface and no signs of detachment nor cracking were observed along the scratch line. Similarly, for samples TiN4-TiN6, although the width of the scratch was quite large, no signs of detachment were observed. However, in the case of sample TiN3, as seen in the backscattered electron image, traces of WC substrate particles were visible along the scratch line, indicating that the coating detached from the surface due to scratching. An image of the steel-based coated product after the scratch test at a lower magnification compared to the other images is shown in *Figure 7i*. In this case, the penetration depth was too high and the stylus progressed practically without resistance along the surface, easily detaching the coating.

4. Conclusions

In evaluating the research results, the main goal was to qualify the coatings primarily for practical usage purposes. The more resistant a coating applied on a tool is, the longer its expected lifespan, in all likelihood leading to a significant reduction in costs. Drawing conclusions from the qualification of coatings formed using various structures and thicknesses through the CVD process, the following can be inferred:

- For tribological model testing of TiN-based coatings, it is necessary to select a static counterpart with a hardness resembling that of the test specimen as if insufficient, the coating may not be detached at all, even when normal loading is increased.
- In terms of tribology, the average surface roughness of the test specimens has a greater impact on the wear volume than their hardness.
- The stability of coatings is not dependent on their thickness but rather on their surface roughness and hardness.
- From a tribological and micromachining perspective, it is much more advantageous to use tools coated by a CVD process that results in sharp, lenticular-like crystals on the surface.
- In the event of long-term usage, it is advisable to develop a coating that includes a support layer between the titanium-based layers.
- Since tribological model tests do not always adequately reflect adhesion of the respective coatings to the surface, it is advisable to conduct supplementary scratch tests.

SYMBOLS

CVD	chemical vapour deposition
EDS	energy-dispersive X-ray spectroscopy
HT-CVD	high-temperature CVD
PS	plasma spray
PVD	physical vapor deposition
SEM	scanning electron microscopy
TiC	titanium carbide
TiCN	titanium carbonitride
TiN	titanium nitride
WC	tungsten carbide
WC-Co	tungsten carbid - cobalt
XRD	X-ray diffraction
Vp	wear volume
D	the diameter of the wear scar on the ball
h	the height of the removed material from the ball
Pd	Penetration depth
R	the original radius of the ball
Ra	average surface roughness
μ	coefficient of friction

Acknowledgements

This work was supported by the TKP2020-NKA-10 project financed under the 2020-4.1.1-TKP2020 Thematic Excellence Programme by the National Research, Development and Innovation Fund of Hungary.

The project 2019-1.1.1-PIACI-KFI-2019-00506 was implemented with financial support provided by the Ministry of Innovation and Technology through the National Research, Development and Innovation Fund. The project was funded under the Market-driven Research and Innovation Projects Support Programme.

REFERENCES

[1] Franklin, S.E; Beuger, J.: A comparison of the tribological behaviour of several wear-resistant coatings, *Surf. Coat. Technol.*, 1992, **54-55**, 459–465, DOI: 10.1016/S0257-8972(07)80066-1

[2] Rebenne, H.E.; Bhat, D.G.: Review of CVD TiN coatings for wear-resistant applications: deposition processes, properties and performance, *Surf. Coat. Technol.*, 1994, **63**(1-2), 1–13, DOI: 10.1016/S0257-8972(05)80002-7

[3] Staia, M.H.; Lewis, B.; Cawley, J.; Hudson, T.: Chemical vapour deposition of TiN on stainless steel, *Surf. Coat. Technol.*, 1995, **76-77**, 231–236, DOI: 10.1016/0257-8972(95)02527-8

[4] Garcia, J.; Pitonak, R.; Weissenbacher, R.; Köpf, A.: Production and characterization of wear resistant Ti(C,N) coatings manufactured by modified chemical vapor deposition process, *Surf. Coat. Technol.*, 2010, **205**(7), 2322–2327, DOI: 10.1016/j.surfcoat.2010.09.013

[5] You, Q.; Xiong, J.; Li, H.; Guo, Z.; Huo, Y.: Study on the microstructure and high temperature friction and wear characteristics of three CVD coated cermets, *Int. J. Refract. Met. Hard Mater.*, 2021, **96**, 105495, DOI: 10.1016/j.ijrmhm.2021.105495

[6] Su, Y.L.; Kao, W.H.: Tribological behavior and wear mechanisms of TiN/TiCN/TiN multilayer coatings, *J. Mater. Eng. Perform.*, 1998, **7**, 601–612, DOI: 10.1361/105994998770347440

[7] Dobrzański, L.A.; Pakuła, D.; Křiž, A.; Soković, M.; Kopač, J.: Tribological properties of the PVD and CVD coatings deposited onto the nitride tool ceramics, *J. Mater. Process. Technol.*, 2006, **175**(1-3), 179–185, DOI: 10.1016/j.jmatprotec.2005.04.032

[8] Polcar, T.; Kubart, T.; Novák, R.; Kopecký, L.; Široký, P.: Comparison of tribological behaviour of TiN, TiCN and CrN at elevated temperatures, *Surf. Coat. Technol.*, 2005, **193**(1-3), 192–199, DOI: 10.1016/j.surfcoat.2004.07.098

[9] Ji, W.; Zou, B.; Liu, Y.; Huang, C.; Guo, P.: Frictional behavior and wear resistance performance of gradient cermet composite tool materials sliding against hard materials, *Ceram. Int.*, 2017, **43**(10), 7816–7826, DOI: 10.1016/j.ceramint.2017.03.096

[10] Rebelo de Figueireiredo, M.; Muratore, C.; Franz, R.; Chromik, R.R.; Wahl, K.J.; Voevodin, A.A; O'Sullivan, M.; Lechthaler, M.; Mitterer C.: In situ studies of $TiC_{1-x}N_x$ hard coating tribology, *Tribol. Lett.*, 2010, **40**(3), 365–373, DOI: 10.1007/s11249-010-9664-7

[11] Boing, D.; de Oliveira, A.J.; Schroeter, R.B.: Evaluation of wear mechanisms of PVD and CVD coatings deposited on cemented carbide substrates applied to hard turning, *Int. J. Adv. Manuf. Technol.*, 2020, **106**(11-12), 5441–5451, DOI: 10.1007/s00170-020-05000-x

[12] Yang, L.; Xiong, J.; Chen, X.; Li, X.; Deng, C.; Zhang, D.; Yi, L.: Study on the growth and wear characters of CVD coating deposited on Ti(C,N)-based cermets with adding different C/N ratios of Ti(C,N) powders, *Ceram. Int.*, 2023, **49**(11), 18023–18034, DOI: 10.1016/j.ceramint.2023.02.255

[13] Zheng, Z.P.; Lin, N.; Zhao, L.B.; Li, X.; He, Y.H.: Fabrication and wear mechanism of Ti(C,N)-based cermets tools with designed microstructures used for machining aluminum alloy, *Vacuum*, 2018, **156**, 30–38, DOI: 10.1016/j.vacuum.2018.07.012

[14] von Fieandt, L.; Larsson, T.; Lindahl, E.; Bäcke, O.; Boman, M.: Chemical vapor deposition of TiN on transition metal substrates, *Surf. Coat. Technol.*, 2018, **334**, 373–383, DOI: 10.1016/j.surfcoat.2017.11.063

[15] Toller, L.; Liu, C.; Holmström, E.; Larsson, T.; Norgen, S.: Investigation of cemented carbides with alternative binders after CVD coating, *Int. J. Refract. Met. Hard Mater.*, 2017, **62**, 225–229, DOI: 10.1016/j.ijrmhm.2016.07.005

[16] Matei, A.A.; Turcu, R.N.; Pencea, I.; Herghelegiu, E.; Petrescu, M.I.; Niculescu, F.: Comparative characterization of the TiN and TiAlN coatings deposited on a new WC-Co tool using a CAE-PVD technique, *Crystals*, 2023, **13**(1), 112, DOI: 10.3390/cryst13010112

[17] Chen, X.; Xu, J.; Xiao, Q.: Cutting performance and wear characteristics of Ti(C,N)-based cermet tool in machining hardened steel, *Int. J. Refract. Met. Hard Mater.*, 2015, **52**, 143–150, DOI: 10.1016/j.ijrmhm.2015.06.006

[18] Peng, Y.; Miao, H.; Peng, Z.: Development of TiCN-based cermets: Mechanical properties and wear mechanism, *Int. J. Refract. Met. Hard Mater.*, 2013, **39**, 78–89, DOI: 10.1016/j.ijrmhm.2012.07.001

[19] ASTM G99-05(2010): Standard test method for wear testing with a pin-on-disk apparatus

[20] ASTM G133-05(2010): Standard test method for linearly reciprocating ball-on-flat sliding wear

[21] Cabral, G.; Ali, N.; Titus, E.; Gracio, J.: Cobalt diffusion in different microstructured WC-Co substrates during diamond chemical vapor deposition, *J. Phase Equilib. Diff.*, 2005, **26**(5), 411–416, DOI: 10.1007/s11669-005-0027-2

[22] Molnár, V., Sztankovics, I.: Analysis of roughness parameters determining tribological properties in hard turned surfaces, *Hung. J. Ind. Chem.*, 2022, **49**(2), 77–84, DOI: 10.33927/hjic-2021-26

[23] Badisch, E.; Fontalvo, G.A.; Mitterer, C.: The response of PACVD TiN coatings to tribological tests with different counterparts, *Wear*, 2004, **256**(1-2), 95–99, DOI: 10.1016/S0043-1648(03)00391-0

[24] Táncsics, F.; Halbritter, E.: PVD coating and up-to-date wear test of hot-forming tools, *Hung. J. Ind. Chem.*, 2012, **40**(1), 19–24, DOI: 10.1515/313

[25] Candido, L.M.; Fais, L.M.G.; Reis, J.M.S.N.; Pinelli, L.A.: Surface roughness and hardness of yttria stabilized zirconia (Y-TZP) after 10 years of simulated brushing, *Rev. Odontol. UNESP*, 2014, **43**(6), 379–383, DOI: 10.1590/1807-2577.1049